INVESTIGATING SLANTED DOUBLE BOUNCE SCATTERING MECHANISMS BASED ON SCATTERING MODELS

Jong-Sen Lee[1,2], Thomas L. Ainsworth[1] and Yanting Wang[1]

[1]Naval Research Laboratory, Washington DC, USA
[2]Computational Physics Inc., Springfield, VA, USA

ABSTRACT

In this paper, we investigate the double bounce radar backscattering from building walls not aligned in the azimuth direction (i.e., slanted double bounce scattering) based on scattering models. We apply the Fresnel equation for reflections from the building wall, and then the bistatic small perturbation model developed by Ulaby for ground scattering. Our analysis indicates that scattering matrix is not symmetrical for the path from radar to wall to ground and back to radar, but adding the reverse path from radar to ground to wall and back to radar makes the scattering matrix symmetrical. The effect on the polarization orientation estimation for an urban scene using L-band E-SAR will be analyzed.

Index Terms— Polarimetric SAR, Radar Polarimetry, Polarization Orientation Estimation.

1. INTRODUCTION

Double bounce backscattering from buildings aligned along azimuth (along track) direction has been well investigated, and its characteristics are similar to scattering from a dihedral. The co-pols are close to 180° out of phase, the cross-pol power are smaller than co-pols, and its polarization orientation rotation (POA) is near zero.. Less known is the scattering characteristics from buildings not aligned in the azimuth direction. We called it "slanted double bounce". The radar signal bounced from the wall at an angle, and scattering back from rough ground. The scattering is significantly different from the typical double bounce. For smooth ground on the scale of radar wavelength, the signal returned to radar could be too small to be detected. On the other hand, for rougher ground, signal can scatter back to radar. Significant cross-pol power could be induced that impedes the target detection and identification using polarimetric SAR. Many algorithms have been proposed to mitigate this effect by enhancing the double bounce scattering power while reducing the cross-pol for easier target classification [1, 2].

It has shown that polarization orientation angle shifts has been induced by the slanted double bounce scattering. Orientation compensation can reduce the cross-pol power, and increase the double bounce power correspondently. Consequently, the orientation angle compensation has been applied to improve the detection of manmade structures in urban areas [1, 2]. Several studies have been devoted to relate empirically the slanted building angle to the estimated orientation angle [3, 4]. This procedure has found applications in polarimetric SAR phase calibration to compensate for the Faraday rotation effect from the ionosphere. However, it lacks the theoretical proof on the validity of the estimated angle of the slanted buildings based on POA, and the estimation could be in error.

In this paper, we initialized a study on the scattering characteristics of slanted double bounce based on scattering models. We apply the Fresnel equation for reflections from the building wall, and then the bistatic small perturbation model for ground scattering (Ulaby, 1986 [5]). We found that the scattering matrix for the signal path from radar to wall to ground and back to radar is not symmetrical – similar to bistatic scattering. However, by adding the reverse path from radar to the ground to wall and back to radar, the scattering matrix becomes symmetrical. The scattering matrix will be analyzed as a function of slanted building angle, radar incidence angle and dielectric constants.

2. SCATTERING MECHANISM OF SLANTED DOUBLE BOUNCE

Just like regular double bounce scattering, the slanted double bounce scattering follows two scattering passes. The first path is from radar to wall to ground and back to radar, and the second path is from radar to ground to wall and back to radar. The difference is that the two scattering matrices for regular double bounce are identical, but, in contrast, they are different for slanted double bounce scattering.

Path #1: Radar – Wall – Ground – Radar

A schematic diagram for the path is shown in Fig. 1. The radar wave travels from radar in the inverse direction of $\hat{\boldsymbol{I}}_1$

with look angle θ . The signal is reflected from the wall, hit the ground, and then scatters back to the radar. The geometry including the H and V polarizations becomes messy. Carefully tracing the signal with polarization vectors in three different coordinate systems is essential to obtain correct solution.

The wall is slanted at an angle α with respect to the x-axis. The normal vector to the wall is $\hat{N}_W$. The local incidence angle to the wall can be easily obtained by

$$\theta_1 = \cos^{-1}(\sin\theta\cos\alpha)$$

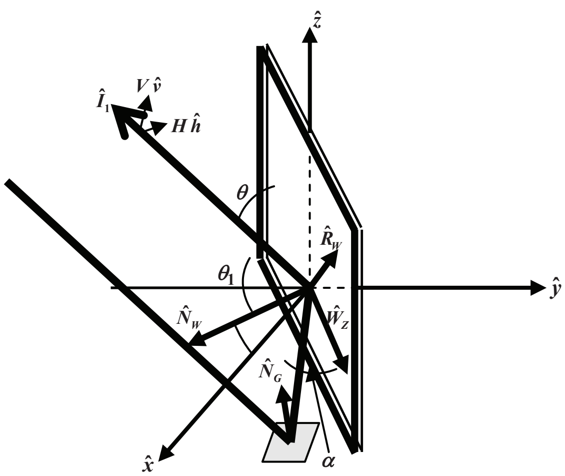

Fig. 1 Schematic diagram of slanted double bounce scattering

It is necessary to convert the signal amplitude H and V from the antenna polarization coordinate ($\hat{h}, \hat{v}$) to the ($\hat{h}_w$ $\hat{v}_w$) coordinate for the convenience of applying the Fresnel equation. The following rotation is required

$$\begin{bmatrix} H_W \\ V_W \end{bmatrix} = \begin{bmatrix} \cos\gamma & -\sin\gamma \\ \sin\gamma & \cos\gamma \end{bmatrix} \begin{bmatrix} H \\ V \end{bmatrix} \qquad (1)$$

where γ is the angle between $\hat{h}$ and $\hat{h}_w$, and it can be obtained by

$$\cos\gamma = \cos\theta\cos\alpha / \sin\theta_1 . \qquad (2)$$

Applying Fresnel reflection coefficient (R_H, R_V), we have the signal reflected from the wall

$$\begin{bmatrix} R_H & 0 \\ 0 & R_V \end{bmatrix} \begin{bmatrix} \cos\gamma & -\sin\gamma \\ \sin\gamma & \cos\gamma \end{bmatrix} \begin{bmatrix} H \\ V \end{bmatrix} \qquad (3)$$

Please note that R_H is negative and R_V is positive.

After reflected from the wall, the polarization coordinates has to be rotate again to the coordinate of the ground. That is from ($\hat{h}_w, \hat{v}_w$) to the ground polarization ($\hat{h}_g , \hat{v}_g$). Here, the ground is assumed to be horizontal that makes the local incidence angle to the rough ground equals to the radar look angle θ . Also the scattering angle from the ground back to radar is also equal to θ . The angle between $\hat{h}$ and $\hat{h}_w$ can be shown is also equals to γ . The rotation is in the same direction as the rotation from radar to wall as shown in (1). This rotation produces the input polarization amplitude to the ground to facilitate applying the small perturbation model of bistatic scattering by Ulaby et al. [5]. Equation (3) becomes

$$\begin{bmatrix} \cos\gamma & -\sin\gamma \\ \sin\gamma & \cos\gamma \end{bmatrix} \begin{bmatrix} R_H & 0 \\ 0 & R_V \end{bmatrix} \begin{bmatrix} \cos\gamma & -\sin\gamma \\ \sin\gamma & \cos\gamma \end{bmatrix} \begin{bmatrix} H \\ V \end{bmatrix} \qquad (4)$$

After the signal bounced from the wall, the small perturbation model for bistatic scattering from ground [5] is then applied. Based on the incidence angle, the scattering angle θ , and the azimuth angle -2α for the signal back to the radar, the FSA scattering matrix can be computed as ($B_{HH}, B_{VH}, B_{HV}, B_{VV}$). Finally, we obtain the scattering matrix in forward scattering alignment (FSA)

$$S^1_{FSA} =$$

$$\begin{bmatrix} B_{HH} & B_{VH} \\ B_{HV} & B_{VV} \end{bmatrix} \begin{bmatrix} \cos\gamma & -\sin\gamma \\ \sin\gamma & \cos\gamma \end{bmatrix} \begin{bmatrix} R_H & 0 \\ 0 & R_V \end{bmatrix} \begin{bmatrix} \cos\gamma & -\sin\gamma \\ \sin\gamma & \cos\gamma \end{bmatrix} \qquad (5)$$

The azimuth angle for the ground bistatic scattering is -2α . We note that, when the incidence angle and the scattering angle are equal, $B_{HV} = -B_{VH}$. It is interesting to note that (5) is not a backscattering matrix in FSA because of $S^1_{HV} \neq -S^1_{VH}$. However, adding the second path to be shown below will make the final scattering matrix correct in symmetry.

Path #2: Radar – Ground – Wall – Radar

Following the similar procedure of Path #1, the reverse path can be shown to obtain the scattering matrix in FSA for path #2,

$$S^2_{FSA} =$$

$$\begin{bmatrix} \cos\gamma & -\sin\gamma \\ \sin\gamma & \cos\gamma \end{bmatrix} \begin{bmatrix} R_H & 0 \\ 0 & R_V \end{bmatrix} \begin{bmatrix} \cos\gamma & -\sin\gamma \\ \sin\gamma & \cos\gamma \end{bmatrix} \begin{bmatrix} B_{HH} & B_{VH} \\ B_{HV} & B_{VV} \end{bmatrix} \qquad (6)$$

The final scattering matrix is the sum of these paths,

$$S_{FSA} = S^1_{FSA} + S^2_{FASA} \qquad (7)$$

The scattering matrix in BSA can be obtained by

$$S_{BSA} = \begin{bmatrix} -1 & 0 \\ 0 & 1 \end{bmatrix} S_{FSA} \qquad (8)$$

After converting (7) into BSA, we found that Eq. (8) is a bona fide scattering matrix because of $S_{HV} = S_{VH}$.

An Illustrated Example

For illustration, we compute the following case: The incidence angle $\theta = 30^\circ$, the wall angle $\alpha = 10^\circ$, the relative dielectric constants for wall and for the ground are $\varepsilon_w = 40$ and $\varepsilon_g = 4$, respectively. Based on our calculation from (5) to (8), the scattering matrix in BSA is

$$S_{BSA} = \begin{bmatrix} -0.596 & 0.047 \\ 0.047 & 0.258 \end{bmatrix} \quad (9)$$

Equation (9) possesses the correct property of a backscattering matrix, namely, $S_{HV} = S_{VH}$. It is interesting to note that, similar to the typical double bounce scattering, S_{HH} and S_{VV} are out of phase and $|S_{HH}| > |S_{VV}|$.

3. EXPERIMENT

The E-SAR L-Band PolSAR data is used for illustration. The original image was decomposed by Freeman and Durden decomposition shown in Fig. 2A. It reveals that the buildings aligned in the flight direction are shown in red, but the slanted buildings are in green indicating strong cross-pol returns. The orientation angle was computed by the circular pol estimator, and is shown in Fig. 2B. To enhance the clarity of city blocks' orientation angle, we have incorporated the span to the display. The image is coded with (Hue, Saturation, Intensity), with Hue ad Saturation coded as color for orientation angle as shown in Fig. 2C, and Intensity by the span.

Fig. 2B clearly shows that many slanted building in the lower half of the image has negative orientation angle in blue color corresponding to negative alpha angle, and the positive orientation angle corresponds to the positive alpha angle in red color located in the upper half part of the image. The buildings in red have opposite slanted angles as those in blue. We will compare the experiment results from those obtained by the proposed scattering models in a coming study.

4. SUMMARY

The backscattering in urban area is a mixture of direct surface scattering from ground, wall, roof and other structure, and slanted double bounce as discussed in this paper. In certain circumstance, it can be difficult to know which scattering mechanism is dominant.

The complexity of double bounce scattering from buildings and manmade targets not aligned in the along-track direction has been investigated using scattering models. To avoid possible errors, we analyze the scattering mechanism based on forward scattering alignment (FSA), and then convert to BSA afterwards. Further analysis is required for its effect on orientation angle estimation that related to the physical orientation of buildings.

(A) Freeman decomposition

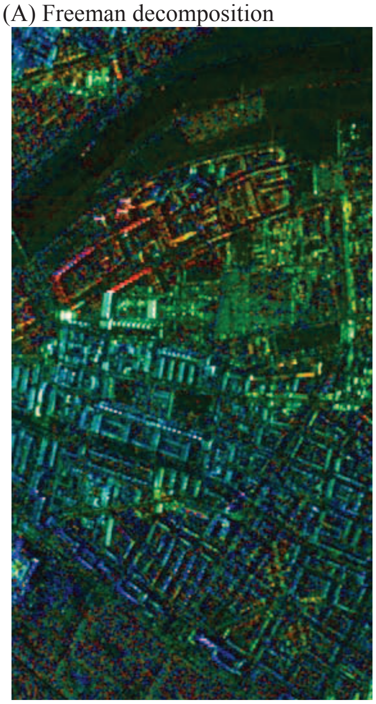

(B) Orientation angle + span

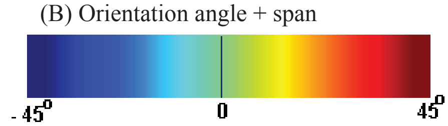

(C) Color label of orientation angle in (B)

Fig. 2 E-SAR L-band PolSAR data of Dresden is used for illustration for POA estimation. The image is displayed with Freeman/Durden decomposition in (A), and the orientation angle enhanced by the span is shown in (B), and *color coded by (C). We observe that double bounce pixels shown in red in (A) have their orientation angle close to zero in (B), whereas buildings not aligned in the along track direction has different POA as shown with different color*

5. REFERENCES

[1] J.S. Lee and T.L. Ainsworth, "The effect of orientation angle compensation on coherency matrix and polarimetric target decomposition," IEEE Trans. on Geoscience and Remote Sensing, vol. 49, no. 1, pp. 43-64, Jan 2011

[2] Y. Yamaguchi, et al., "Four-component scattering power decomposition with rotation of coherency matrix," IEEE Trans. on Geoscience and Remote Sensing, vol. 49, no. 6, pp. 2251-2258, June 2011.

[3] H. Kimura, K.P. Papathanassiou and I. Hajnsek, "Polarization Orientation Effect in Urban Areas on PolSAR Data," *Proceedings of IGARSS 2005*, pp. 4863-4867, Seoul, July 2005.

[4] K. Irebe and M. Sato, "Analysis of Polarization Orientation Angle Shifts by Artificial Structures," *IEEE Trans. on Geoscience and Remote Sensing,* vol.45, no.11, pp. 3417-3425, 2007.

[5] F.T. Ulaby, R.K. Moore and A.K. Fung, Microwave Remote Sensing: Active and Passive, Vol. III, From Theory to Applications, Artech House, 1986.